Real-Time Interrogation of a Linearly Chirped Fiber Bragg Grating Sensor for Simultaneous Measurement of Strain and Temperature

Weilin Liu, *Student Member, IEEE*, Wangzhe Li, *Student Member, IEEE*, and Jianping Yao, *Senior Member, IEEE*

Abstract—We propose and demonstrate a novel approach to real-time interrogation of a high-birefringence linearly chirped fiber Bragg grating (Hi-Bi LCFBG) for simultaneous measurement of strain and temperature based on chirped microwave pulse compression with increased resolution and signal-to-noise ratio (SNR). A theoretical analysis is developed, which is validated by an experiment. The experimental results show that the proposed system can provide a resolution better than $\pm 1.2\,^{\circ}\mathrm{C}$ and $\pm 13.3\,\mu\varepsilon$ at an interrogation speed of 48.6 MHz.

Index Terms—Chirped fiber Bragg grating (CFBG), chirped microwave pulse, interrogation, sensor, wavelength-to-time mapping.

I. INTRODUCTION

FIBER Bragg grating (FBG) sensors have been investigated extensively in the last few decades. Among the numerous applications, an FBG sensor is particularly useful for strain or temperature sensing. Since both the strain and temperature information is encoded in an FBG as a wavelength shift, special measures must be taken to separate the two measurands. A solution is to use a second FBG that is isolated from strain as a temperature reference, but this approach will increase the complexity of the system. Therefore, it is desirable that a single FBG is employed to perform both strain and temperature measurement. A number of approaches have been proposed [1]–[4]. The fundamental principle of these approaches is to use a sensing element that can differentiate the strain and the temperature information, such as the use of differently ion-doped FBGs [1], dual-diameter FBGs [2], hybrid FBGs/long-period gratings [3], or a tilted FBG [4]. The interrogation [1]–[4] is performed using both optical power and wavelength shift detection to distinguish the cross-sensitivity effect between the strain and temperature, but the interrogation speed is still low due to the low speed of optical spectrum detection. It is highly desirable to design an interrogation system for simultaneous and real-time monitoring of strain and temperature [5], [6]. In this letter, we propose a novel technique to real-time interrogation of a high-birefringence linearly chirped fiber Bragg grating (Hi-Bi LCFBG) for simultaneous measurement of strain and temperature. In the proposed
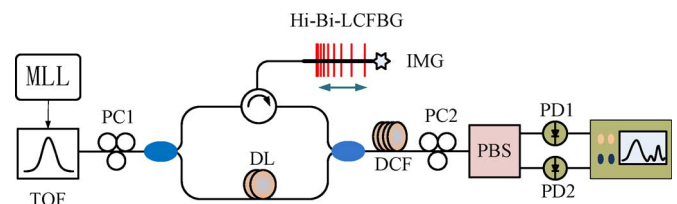
Fig. 1. Schematic of the proposed sensor interrogation system.

system, the strain and temperature information is encoded in the Hi-Bi LCFBG as Bragg wavelength shifts. The Hi-Bi LCFBG is incorporated in one arm of a Mach–Zehnder interferometer (MZI). Due to the birefringence in the Hi-Bi LCFBG, the MZI has two spectral responses along the fast and slow axes with each having an increasing free spectral range (FSR). If an ultrashort optical pulse is sent to the MZI, the spectrum of the ultrashort optical pulse is shaped. Two shaped spectra are obtained which are mapped to two chirped microwave waveforms in a dispersive fiber. By using chirped microwave pulse compression, two correlation peaks with the locations containing the strain and temperature information are obtained. In addition, since the correlation operation here is equivalent to matched filtering, the signal-to-noise ratio (SNR) is increased. A theoretical analysis is developed, which is validated by an experiment.

II. PRINCIPLE

Fig. 1 shows the schematic of the proposed interrogation system. An ultrashort pulse train generated by a mode-locked laser (MLL) source is sent to an MZI through a tunable optical filter (TOF). The TOF here is used to control the spectral width of the ultrashort pulse to the MZI. A Hi-Bi LCFBG is incorporated in the upper arm of the MZI. Due to the birefringence in the Hi-Bi LCFBG, two shaped spectra that are orthogonally polarized are obtained and are sent to a dispersion compensating fiber (DCF). The DCF is serving as a dispersive element to achieve linear wavelength-to-time (WTT) mapping [7]. The orthogonally polarized temporal waveforms obtained at the output of the DCF are separated by a polarization beam splitter (PBS), and then applied to two photodetectors (PDs). A polarization controller (PC1) before the MZI is adjusted such that the polarization direction of the light wave entering the Hi-Bi LCFBG is aligned at an angle of 45° with the fast axis. At the output of the MZI, two orthogonally polarized spectrum-shaped pulses are generated which are mapped to the temporal domain in the DCF, with both the strain and

temperature information being encoded in the temporal wave-forms. The two temporal waveforms are separated by the PBS and detected by the PDs. The microwave waveforms are then sent to a digital signal processor to perform correlation with a special reference waveform. The locations of the correlation peaks would reveal the strain and temperature information.

For the MZI, two transfer functions corresponding to the light wave traveling along the fast and slow axes of the Hi-Bi LCFBG are given [8],

$$\begin{bmatrix} H_f(\omega) \\ H_s(\omega) \end{bmatrix} \cong \frac{\sqrt{2}}{2} \begin{bmatrix} \sqrt{1 + \cos\left(\frac{\ddot{\Phi}_v \omega^2}{2} + \omega \Delta t_f\right)} \\ \sqrt{1 + \cos\left(\frac{\ddot{\Phi}_v \omega^2}{2} + \omega \Delta t_s\right)} \end{bmatrix} \\ \exp\left[-j\omega t_1 + \frac{j\left(a_0\omega^2 - \omega \Delta t\right)}{2}\right] \quad (1)$$

where $\ddot{\Phi}_v = d^2\theta(\omega)/d\omega^2\big|_{\omega=\omega_0}$ (ps^2) is the first-order disper-sion coefficient of the LCFBG, t_1 is the time delay of the upper arm, and Δt_f, Δt_s are the time delay differences between the two arms of the unbalanced MZI with respect to the fast and slow axes of the Hi-Bi LCFBG.

In (1), the first-order dispersion coefficient $\ddot{\Phi}_v$ determines the frequency chirp rate of the generated waveforms. A higher dis-persion of the Hi-Bi LCFBG would give a higher chirp rate. It can be seen that the time delay differences Δt_f and Δt_s are re-sulted from two sources. 1) The optical path difference of the single-mode fibers (SMFs) in the two arms contributes a con-stant time delay difference to Δt_f and Δt_s. The constant time delay difference is given as $n_{eff}\Delta l_0$ where n_{eff} is the effec-tive refractive index of the SMFs, and Δl_0 is the physical length difference between the SMFs in the two arms. 2) The optical paths of the Hi-Bi LCFBG are strain- and temperature-depen-dent, which are given as $2\Delta\lambda n_f/C$ and $2\Delta\lambda n_s/C$, where n_f and n_s are respectively the refractive indices of the fast and slow axis , C (nm/cm) is the chirp parameter of the Hi-Bi LCFBG, and $\Delta\lambda_f = \lambda_0\{(1-\rho_\alpha)\Delta\varepsilon + [\alpha + (1/n_f)(dn_f/dT)]\Delta T\}$, $\Delta\lambda_s = \lambda_0\{(1-\rho_\alpha)\Delta\varepsilon + [\alpha + 1/n_s(dn_s/dT)]\Delta T\}$, where $\Delta\varepsilon$ is the strain difference applied to the Hi-Bi LCFBG, ρ_α and α are the photoelastic coefficient and the thermal expansion co-efficient of the Hi-Bi LCFBG [8], n_f and n_s are the refractive indices of the fast and slow axes, and ΔT is the temperature change. Therefore, Δt_f and Δt_s can be written as

$$\begin{bmatrix} \Delta t_f \\ \Delta t_s \end{bmatrix} = \frac{n_{eff}\Delta l_0}{c} + \frac{2\lambda_0}{Cc}(1-\rho_\alpha)\Delta\varepsilon \\ + \frac{2\lambda_0}{Cc}\Delta T \begin{bmatrix} \alpha + \frac{1}{n_f}\frac{dn_f}{dT} \\ \alpha + \frac{1}{n_s}\frac{dn_s}{dT} \end{bmatrix} \quad (2)$$

where c is the speed of light in vacuum. It can be seen from (1) and (2), Δt_f and Δt_s determine the FSRs of the MZI due to the sensing information change. Thus, the MZI would accomplish two functions: spectral shaping for chirped pulse generation and sensing information encoding.

Since the first-order dispersion $\ddot{\Phi}_v$ in (1) is large and cannot be ignored, the dispersion from the Hi-Bi LCFBG can be com-bined with the dispersion of the DCF, to perform jointly the WTT mapping. The total dispersion for the WTT mapping is

$\ddot{\Phi} = (\ddot{\Phi}_v/2) + \ddot{\Phi}_D$, where $\ddot{\Phi}_D$ is the first-order dispersion of the DCF. The temporal waveforms at the output of the PDs are given by [7]

$$P\begin{bmatrix} s_f(t) \\ s_s(t) \end{bmatrix} \\ \cong T\left(\frac{t}{\ddot{\Phi}_\lambda}\right) \begin{bmatrix} 1 + \cos\{\pi k t[t + f_0 + f_1\Delta T + g\Delta\varepsilon]\} \\ 1 + \cos\{\pi k t[t + f_0 + f_2\Delta T + g\Delta\varepsilon]\} \end{bmatrix} \quad (3)$$

where $\ddot{\Phi}_\lambda = -(2\pi c/\lambda^2)\ddot{\Phi}$ (ps/nm), $T\left(t/\ddot{\Phi}_\lambda\right)$ is a window function determined by the transfer function of the tun-able optical filter, $k = 2n_{eff}/\left(C\lambda_0^2\ddot{\Phi}_\lambda^2\right)$, $f_0 = C\ddot{\Phi}_\lambda\Delta l_0$, $g = 2\ddot{\Phi}_\lambda\lambda_0(1-\rho_\alpha)$, $f_1 = 2\ddot{\Phi}_\lambda\lambda_0[\alpha + (1/n_f)dn_f/dT]$, and $f_2 = 2\ddot{\Phi}_\lambda\lambda_0[\alpha + (1/n_s)dn_s/dT]$.

A special reference waveform with the same chirp rate but a frequency range corresponding to the Hi-Bi LCFBG experi-encing the largest and smallest wavelength shift is built to per-form the correlation [7], which is given by

$$s_r(t) = rect\left(\frac{t}{T_1}\right)\cos\left(2\pi f_0 t + \pi k t^2\right). \quad (4)$$

The correlation peak positions between the waveforms in (3) and the reference in (4) are τ_f and τ_s, and the strain and tem-perature information can be calculated by [7]

$$\begin{bmatrix} \Delta T \\ \Delta\varepsilon \end{bmatrix} = -2\begin{bmatrix} f_1 & g \\ f_2 & g \end{bmatrix}^{-1}\begin{bmatrix} \tau_f \\ \tau_s \end{bmatrix}. \quad (5)$$

III. EXPERIMENT

An experiment based on the setup shown in Fig. 1 is imple-mented. Due to the lack of a Hi-Bi LCFBG, in the experiment, we use a regular LCFBG and a polarization maintaining fiber (PMF), which function equivalently as a Hi-Bi LCFBG. In the experiment, a transform-limited ultrashort Gaussian pulse train at a repetition rate of 48.6 MHz from an MLL source (IMRA Femtolite 780) is sent to a tunable optical filter (TOF). A pulse in the pulse train has a full-width at half-maximum (FWHM) of 394 fs and a center wavelength of 1558.3 nm. The TOF has a bandwidth of 0.58 nm. The ultrashort pulse after the TOF is sent to the MZI. An LCFBG, which is 11.5 cm long with a center Bragg wavelength of 1560.8 nm and a dispersion of -1347 ps/nm, is incorporated in the upper arm of the MZI. The lower arm of the MZI has a tunable time delay line and a length of PMF with a beat length of 3.75 mm. Before applying strain or heating to the LCFBG, we tune PC1 to make the pulse polarization direction align at 45° with respect to the fast axis of the PMF to make the interference pattern have the highest visibility. A length of DCF is connected after the MZI to per-form WTT mapping. The value of dispersion is -948 ps/nm, which is selected to ensure that the chirped pulse is not too fast to be detected by the PDs. At room temperature (25 °C), the time delay in the lower arm is tuned such that the MZI has a spectral response corresponding to a linearly chirped waveform with a central frequency of zero and a chirp rate of -0.068 GHz/ps for $t < 0$ and 0.068 GHz/ps for $t > 0$, as shown in Fig. 2(a).

When a strain is applied or the temperature is changed, the FSRs of the MZI will change, and the shaped spectra will also change. Two linearly chirped microwave waveforms with their
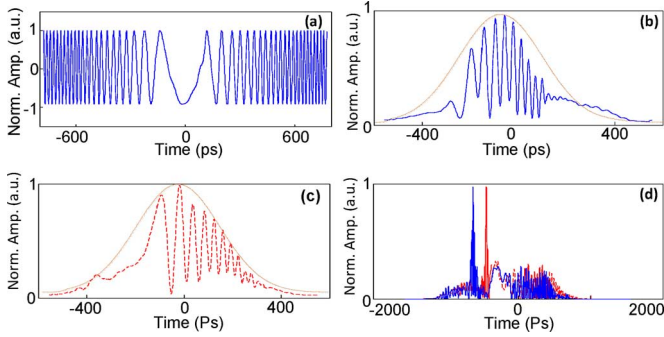
Fig. 2. Experimental results. (a) The special reference waveform. A linearly chirped microwave waveform corresponding to the polarization direction of the ultrashort pulse aligned with (b) the fast axis and (c) the slow axis, when a strain of 50 $\mu\varepsilon$ is applied to the LCFBG at 25 °C. (d) Correlation of the waveforms shown in (b) and (c) with the special reference waveform.
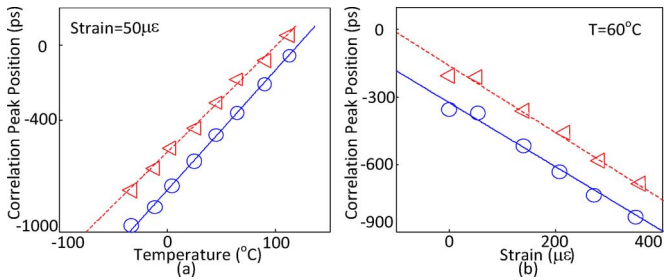

Fig. 3. Experimental results. (a) Correlation peak position versus the temperature for a given strain of 50 $\mu\epsilon$. (b) Correlation peak position versus the applied strain for a temperature of 60 °C. The triangular and circles indicate the experimental data corresponding to the polarization direction of the ultrashort pulse aligned with the fast axis and slow axis, respectively.

instantaneous frequencies indicating the wavelength shift of the LCFBG and the phase difference induced by the PMF is generated at the output of the PDs, which are sent to a digital signal processor for pulse compression. The strain and temperature information are obtained by solving (5).

Fig. 2(b) and (c) shows two linearly chirped microwave waveforms corresponding to the polarization direction of the ultrashort pulse aligned with the fast axis and slow axis respectively when the strain is 50 $\mu\varepsilon$ and the temperature is 25 °C. The correlation of the two linearly chirped microwave waveforms with the special reference waveform given in Fig. 2(a) is shown in Fig. 2(d). It can be seen that the waveforms are highly compressed. The locations of the two peaks indicate the wavelength shifts of the LCFBG and the phase difference due to the birefringence of the PMF. In our experiment, the relationship between the strain or temperature and correlation peak positions is measured, which is shown in Fig. 3. The fitted curves are given by

$$\begin{bmatrix} \Delta T \\ \Delta \varepsilon \end{bmatrix} = \begin{bmatrix} 1.3152°\text{C/ps} & -1.3152°\text{C/ps} \\ 7.6242\ \mu\varepsilon/\text{ps} & -8.4927\ \mu\varepsilon/\text{ps} \end{bmatrix} \begin{bmatrix} \tau_f \\ \tau_s \end{bmatrix}. \quad (6)$$

Equation (6) is used to predict the strain and temperature simultaneously applied to the LCFBG and PMF. For a measurement range of 120 °C and 400 $\mu\varepsilon$, the maximum experimental errors obtained are ± 1.2 °C and ± 13.3 $\mu\epsilon$. Compared with the results reported in [1], where the experimental errors are ± 2.2 °C and ± 18.4 $\mu\epsilon$, the approach here clearly demonstrates an increased accuracy. The sensitivities of the proposed system are also measured, which are 6.4 ps/°C and 1.5 ps/$\mu\varepsilon$. Since the WTT mapping enables real-time sensing for a simultaneous measurement of strain and temperature, the interrogation speed is determined by the repetition rate of the MLL, which is 48.6 MHz in this demonstration.

IV. CONCLUSION

We have proposed and experimentally demonstrated a new approach to measuring strain and temperature simultaneously with an increased resolution and SNR. The key device in the system is the MZI that was designed to include a Hi-Bi LCFBG in one arm, which enables the encoding of both the strain and temperature information in the generated chirped microwave waveforms. By correlating the temporal waveforms with a special reference waveform, two correlation peaks with the locations indicating the strain and temperature induced wavelength shifts of the Hi-Bi LCFBG was obtained.

REFERENCES

[1] P. M. Cavaleiro, F. M. Araujo, L. A. Ferreira, J. L. Santos, and F. Farahi, "Simultaneous measurement of strain and temperature using Bragg gratings written in germanosilicate and Boron-codoped germanosilicate fibers," *IEEE Photon. Technol. Lett.*, vol. 11, no. 12, pp. 1635–1637, Dec. 1999.

[2] S. W. James, M. L. Dockney, and R. P. Tatam, "Simultaneous independent temperature and strain measurement using in-fiber Bragg grating sensors," *Electron. Lett.*, vol. 32, no. 12, pp. 1133–1134, Jun. 1996.

[3] H. J. Patrick, G. M. Williams, A. D. Kersey, J. R. Pedrazzani, and A. M. Vengsarkar, "Hybrid fiber Bragg grating/long period fiber grating sensor for strain and/temperature discrimination," *IEEE Photon. Technol. Lett.*, vol. 8, no. 9, pp. 1223–1223, Sep. 1996.

[4] Y. Miao, B. Liu, and Q. Zhao, "Simultaneous measurement of strain and temperature using single tilted fibre Bragg grating," *Electron. Lett.*, vol. 44, no. 21, pp. 1242–1243, Oct. 2008.

[5] E. Udd, W. L. Schulz, J. Seim, M. Morrell, T. Weaver, J. Bush, and G. Adamovsky, "Fiber optic distributed sensing systems for harsh aerospace environments," in *Industrial and Commercial Applications of Smart Structures Technologies, Proc. SPIE*, J. H. Jacobs, Ed., 1999, vol. 3674, pp. 136–147.

[6] F. Yang, D. He, T. Wang, and Y. Wang, "The real-time safety monitoring of railway condition by FBG sensor," in *Proc. 9th Int. Conf. Electronic Measurement & Instruments*, 2009, pp. 1032–1035.

[7] W. Liu, M. Li, C. Wang, and J. P. Yao, "Real-time interrogation of a linearly chirped fiber Bragg grating sensor based on chirped pulse compression with improved resolution and signal-to-noise ratio," *J. Lightw. Technol.*, vol. 29, no. 9, pp. 1239–1247, May 1, 2011.

[8] A. D. Kersy, M. A. Davis, H. J. Patrick, M. LeBlanc, K. P. Koo, C. G. Askins, M. A. Putnam, and E. J. Friebele, "Fiber grating sensors," *J. Lightw. Technol.*, vol. 15, no. 8, pp. 1442–1463, Aug. 1997.